https://doi.org/10.14669/AM/177006

VIBRATION IN THE SYSTEM OF THE BIRFIELD-RZEPPA CONSTANT VELOCITY UNIVERSAL JOINT

ZBIGNIEW DZIOPA[1]

Abstract

The paper presents the analysis of the motion of the intermediate element in the Birfield–Rzeppa joint. The joint is applied, among others, in automotive vehicles as an element of the drive shaft. The cage along with the balls form the intermediate element of the joint. The vibration of the element is activated during the drive shaft rotation. The vibration is enforced kinematically by the mechanism constraints. The constraints are determined by the assumed clutch geometry. The aim of the paper is to determine the variability course of the kinematic quantities characterizing the intermediate element motion of the Birfield–Rzeppa constant velocity universal joint. If the transmission function and the second position function of the clutch lead to the fluctuation of the angular velocity value and the angular acceleration of the cage along with the balls, then vibration is generated within the joint. The paper shows that drive shaft interference can be reduced by using a vibration reduction system. The article does not present an analysis aimed at reducing vibrations. Only the need for its use in the case of serious disturbances has been demonstrated.

Keywords: constant velocity universal joint; Birfield–Rzeppa joint; vibration

1. Introduction

The Birfield–Pzeppa joint is a widely used spatial mechanism nowadays [4], Figure 1. The clutch is applied in live axle of the automotive vehicles with the independent suspension as an element of the articulated drive shaft [1, 3, 6] and [7]. During the vehicle motion the input resulting from the road surface is transferred onto the wheel–body assembly. Relative displacement occurring in the assembly effects in non–axiality of shafts which are the units of the articulated axle shaft. It means that the axle shaft takes different positions ($\delta = \mathrm{var}$), changing in time. The refraction angle of the shaft axle δ connected with a clutch reaches

[1] Department of Automotive Vehicles and Transportation, Faculty of Mechatronics and Mechanical Engineering, Kielce University of Technology, al. Tysiąclecia Państwa Polskiego 7, 25-314 Kielce, Poland, e-mail: zdziopa@tu.kielce.pl, ORCID: 0000-0002-9135-6306.

https://doi.org/10.14669/AM/177006

the highest values in automotive vehicles with the frontal live axle. It occurs while changing the driving direction. The Birfield–Rzeppa joint is also applied in mechanical engineering as an element compensating for the non–axiality of the connected shafts.

The literature discussing this type of joint is extremely concise. The authors approaching the subject focus in their studies on the presentation of the empirical conclusions and the information relating to the constructional characteristic of the joint [14, 15].

The kinematics of the constant velocity joint at various angles were analyzed by, among others: [12, 16, 17]. The dynamics analysis in terms of structural synthesis or analysis of the energy efficiency of the junction was dealt with by [9, 13, 18]. In [18], the influence of some significant dimensional and geometric errors on the kinematic and dynamic parameters of the Rzepp automotive ball joint was examined. Most researchers, when analyzing the efficiency of the Rzepp joint, focus on the contact of the balls with the ball groove. A different approach to this issue was presented by Yamamoto, Matsuda and Okano [11]. It was found that 70% of the friction losses in Rzepp joints result from internal friction caused by the contact of the balls with the cage. An analytical approach to the efficiency of the Rzepp joint is also presented in [1].

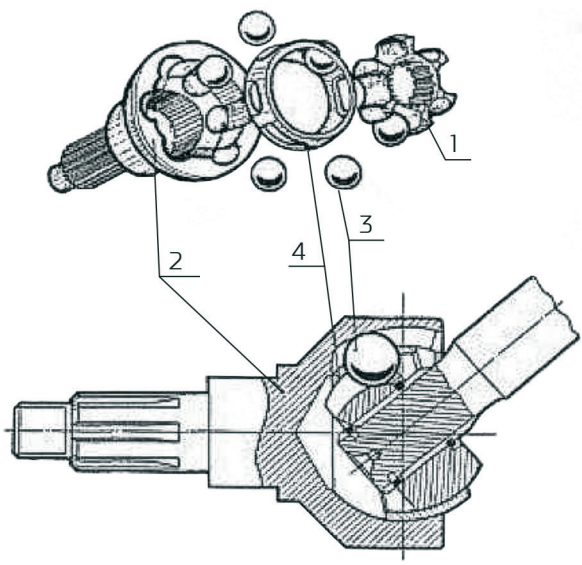

Fig. 1. Birfield–Rzeppa constant velocity joint (1–hub, 2–head, 3–balls, 4–cage) [4]

The theoretical analysis makes it easier to apply the mechanism deliberately in a particular assembly. Defining the kinematic, force–dynamic and dynamic properties allows for optimizing the location of the individual elements of the joint in different operating conditions

https://doi.org/10.14669/AM/177006

[5, 10, 11]. At the same time it reveals the causes of vibrations generated within the assembly. Owing to that fact it is possible to counteract the adverse phenomenon.

The parametric vibrations, which are enforced kinematically, are induced in the discussed joint. They result from the constraints occurring within the mechanism, which are defined by the accepted geometry of the joint. The authors of studies on double-cross joint explicitly assume that the intermediate element is the cause of torsional and bending vibrations in the assembly. Even in the case of uniform rotary motion realized by the drive shaft the intermediate element still turns with the angular acceleration of the fluctuation type. It means that the Birfield-Rzeppa joint, being an element of the power transmission system, may become the source of vibration. The vibrations generated in such a system decrease its durability as well as reliability. Their occurrence is particularly dangerous in transmission systems of high power and rotational speed.

The aim of the paper is to determine the variability course of selected kinematic values characterizing the motion of the homokinetic intermediate element of the Birfield-Rzeppa joint. If the transmission function and the second position function of the clutch induce fluctuation of the angular velocity value and the angular acceleration of the cage along with the balls, then vibrations are generated within the joint.

2. The Physical Model of the Birfield-Rzeppa Joint

Designation

$f(\phi_1)$ – system position function: drive shaft (1) – cage for the balls [radian]
$f'(\phi_1)$ – system transmission function: drive shaft (1) – cage for the balls
$f''(\phi_1)$ – second function of the system position: drive shaft (1) – cage for the balls [1/radian]
$\vec{r}_3$ – vector determining the position of the ball [m]
$\vec{V}_A$ – linear velocity of the ball [m/s]
$\vec{a}_A$ – linear acceleration of the ball [m/s^2]

The actual Bierfield-Rzeppa joint is a sophisticated mechanism which has to be made with extreme accuracy and precision. It refers especially to the proper profile of the guides along which the balls travel. In order to analyze the clutch motion a specially formulated model was applied as in Figure 2. The head with the external grooves for the balls is modeled with a fork and guides P_1. The hub with the internal grooves for the balls is modeled with a fork and the guides P_2. The guides P_1 i P_2 lie in the fork plane of the proper shaft (1) and shaft (2). The balls are modeled with rings (e.g. p.A), and the ball cage include P (the clamping ring).

https://doi.org/10.14669/AM/177006

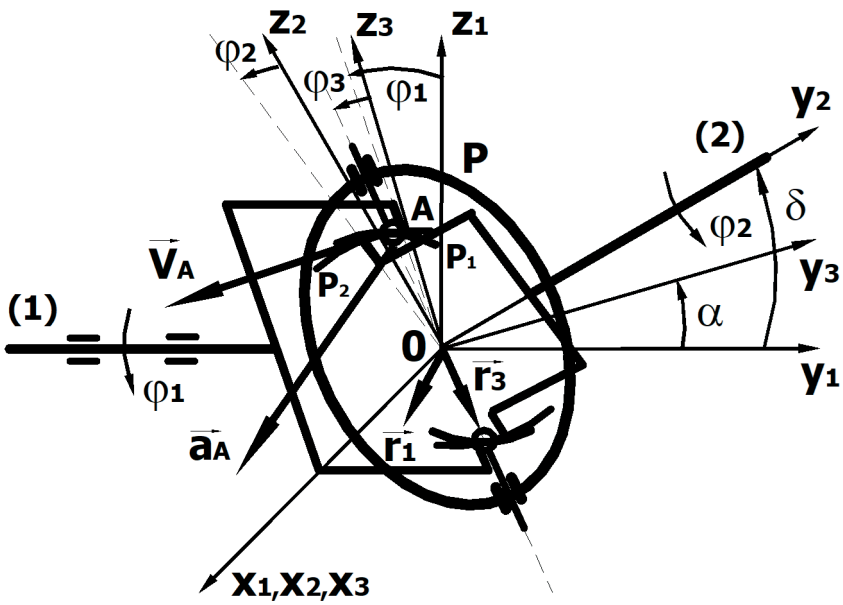

Fig. 2. Birfield–Rzeppa joint model

The mechanism formulated in such a way will be examined in the plane determined by the axis of the drive shaft (1) and the driven shaft (2). The refraction angle of the shaft axis may be defined by one angle δ. We assume that all the sections of the jointed shaft as well as the clutch itself are perfectly rigid:

$$\varphi_1' = \varphi_1'' = \varphi_1 \phi_2' = \phi_2'' = \phi_2 \tag{1}$$

and, the refraction angle of the shafts axles is invariable:

$$\delta = const \tag{2}$$

where:

$\phi_1' = \phi_1''$ – rotation angles of the initial and final sections of the drive shaft
$\phi_2' = \phi_2''$ – rotation angles of the initial and final sections of the driven shaft

The motion of the individual units of the clutch are examined with reference to Cartesian orthogonal right-handed coordinate system. The initial position of the drive shaft, i.e. for $\phi_1\ (t = 0) = 0$, is defined by the inertial coordinate system $0x_1y_1z_1$. For the moment of time $t = 0$ the axis $0y_1$ is directed along the shaft axle (1), and the axis $0z_1$ is in the shaft fork plane (1). The initial position of the driven shaft, i.e. for $\phi_2\ (t = 0) = 0$, is defined by the inertial coordinate system $0x_2y_2z_2$. For the moment of time $t = 0$ the axis $0y_2$ is directed along the shaft axle

https://doi.org/10.14669/AM/177006

(2), and the axis $0z_2$ is in the shaft fork plane (2). The initial position of the clamping ring P, i.e. for $\phi_3\ (t = 0) = 0$, is determined by the inertial coordinate system $0x_3y_3z_3$. For the moment of time $t = 0$ the axis $0y_3$ is perpendicular to the plane π of the rotation of the clamping ring P and inclined towards the axis $0y_1$ at the angle α, and the axis $0z_3$ overlap with the straight line $0A$. 0 is the intersection point of the drive shaft axle and the driven shaft axle.

3. The kinematic condition of the Birfield–Rzeppa joint homokinetism

The kinematic condition of homokinetism is the necessary condition for the constant velocity of the Birfield–Rzeppa joint. In order to define it one must determine the joint position function, which in this case represents the dependence of the driven shaft rotation angle ϕ_2 on the drive shaft rotation angle ϕ_1:

$$\phi_2 \rightleftarrows f(\phi_1) \tag{3}$$

The characteristic geometric locus of the discussed mechanism is the straight line $0A$, owing to its position in the so-called constant velocity plane. The above-mentioned straight line is the intersection edge of the plane π_1, in which lie the guides P_1, with the plane π_2, in which lie the guides P_2.

The straight line $0A$ in the coordinate system $0x_1y_1z_1$ is defined by the following analytical dependencies:

$$\begin{cases} \cos\phi_1\, x_1 - \sin\phi_1\, z_1 = 0 & (4) \\ \cos\phi_2\, x_1 + \sin\delta \sin\phi_2\, y_1 - \cos\delta \sin\phi_2\, z_1 = 0 & (5) \end{cases}$$

where:
(4) – equation of the plane π_1 in the coordinate system $0x_1y_1z_1$
(5) – equation of the plane π_2 in the coordinate system $0x_1y_1z_1$

If we assume that:

$$\vec{r}_1 \perp \pi_1 \quad \text{and} \quad \vec{r}_2 \perp \pi_2 \tag{6}$$

Then the vectors $\vec{r}_1$ and $\vec{r}_2$ are perpendicular to the straight line $0A$, and the vector product

$$\vec{r}_3 = \vec{r}_1 \times \vec{r}_2 \text{where: } |\vec{r}_1| = |\vec{r}_2| = r \cap |\vec{r}_3| = r_3 = r^2 \tag{7}$$

determines the vector $\vec{r}_3$, which is parallel to the straight line $0A$.

https://doi.org/10.14669/AM/177006

On the basis of the dependencies (4), (5), (6) and (7) we receive the coordinates of the vector $\vec{r}_3$ in the coordinate system $0x_1y_1z_1$:

$$\vec{r}_3\left(r_{3x_1}, r_{3y_1}, r_{3z_1}\right) \tag{8}$$

$$r_{3x_1} = r_3 \sin\delta \sin\phi_1 \sin\phi_2$$

$$r_{3y_1} = r_3(\cos\delta \cos\phi_1 \sin\phi_2 - \sin\phi_1 \cos\phi_2)$$

$$r_{3z_1} = r_3 \sin\delta \cos\phi_1 \sin\phi_2$$

After selecting the proper value ofrthe vector $\vec{r}_3$ determines the position of point A.

The plane π of clamping ring rotation P in the coordinate system $0x_1y_1z_1$ is determined by the following equation:

$$\cos\alpha\, y_1 + \sin\alpha\, z_1 = 0 \tag{9}$$

On the basis of the dependencies (8) and (9) we receive the analytical equation of the geometric constraints imposed onto the mechanism motion:

$$tg\phi_2 = \frac{tg\phi_1}{tg\alpha \sin\delta + \cos\delta} \tag{10}$$

Hence:

$$\phi_2 = arctg\left[\frac{tg\phi_1}{tg\alpha \sin\delta + \cos\delta}\right] = f(\phi_1) \tag{11}$$

The equation (11) is the function of the Birfielda–Rzeppa joint position. The function allows for determining the kinematic condition for homokinetism. As a result of trigonometric considerations one can state that the condition is fulfilled for the following dependence:

$$\alpha = \frac{\delta}{2} \tag{12}$$

Therefore the position of the constant velocity plane is determined explicitly with the equation:

$$\cos\frac{\delta}{2} y_1 + \sin\frac{\delta}{2} z_1 = 0 \tag{13}$$

If at every moment of time t the equation of the plane π will meet the dependence (13) then the Birfielda–Rzeppa joint will be the homokinetic clutch. The plane π with so determined position, from the point of view of mechanisms theory, is treated as a constant velocity plane. The clamping ring P motion in the plane π should be guaranteed by the proper geometry of the clutch. Two guides P_1 and P_2 do not satisfy this requirement, because the clamping ring P rotation is possible round the straight line $0A$, constituting local mobility. It is only the

https://doi.org/10.14669/AM/177006

application of at least three guides that provide the right position of the mechanism units. It results from retaining the constant velocity condition for the mechanism with only one active unit. In the actual structure there are six guides along which the balls roll setting the cage in the constant velocity plane.

4. The dynamically enforced condition for the homokinetism of the Birfield–Rzeppa joint

If the kinematic condition for homokinetism is fulfilled then the sufficient condition for the constant velocity of the Birfield–Rzeppa joint is the observation of the dynamically enforced condition [2]. In order to determine the sufficient condition one must define the function $f(\phi_1,\phi_2)$, which in this case represents the dependence between the passive torsional moment $-\vec{M}_{s2}$ shaft [2], and the active torsional moment $\vec{M}_{s1}$ shaft [1]:

$$M_{s2} \rightleftarrows f(\phi_1,\phi_2) M_{s1} \tag{14}$$

The virtual dislocation rule will be used for determining the dependence [14]. The analysis of the system load shows that there are two generalized forces, which should provide the system with the state of equilibrium. Therefore the prepared work is defined by the following equation:

$$\delta A = M_{s1}\delta\phi_1 - M_{s2}\delta\phi_2 = 0 \tag{15}$$

Hence

$$M_{s2} = \frac{\delta\phi_1}{\delta\phi_2} M_{s1} \tag{16}$$

On the basis of the dependencies [10] the analytical equation of finite constraints imposed on the stationary holonomic system has the form:

$$f(\vec{r}_3) = tg\phi_1 - (tg\alpha \sin\delta + \cos\delta) tg\phi_2 = 0 \tag{17}$$

Knowing the equation of the geometric constraints one may proceed to determine the dependence between the virtual dislocations $\delta\phi_1$ and $\delta\phi_2$. For this purpose we can use the following homogenous equation:

$$\frac{\partial f(\vec{r}_3)}{\partial\phi_1}\delta\phi_1 + \frac{\partial f(\vec{r}_3)}{\partial\phi_2}\delta\phi_2 = 0 \tag{18}$$

On the basis of the dependencies [17] and [18] we receive the function which represents the dependence between the passive torsional moment and active torsional moment:

https://doi.org/10.14669/AM/177006

$$\frac{\delta\phi_1}{\delta\phi_2} = \frac{(tg\alpha\, sin\,\delta + cos\,\delta)\, cos^2\,\phi_1}{cos^2\,\phi_2} = f(\phi_1, \phi_2) \tag{19}$$

Hence:

$$M_{s2} = \frac{(tg\alpha\, sin\,\delta + cos\,\delta)\, cos^2\,\phi_1}{cos^2\,\phi_2} M_{s1} \tag{20}$$

The function $f(\phi_1,\phi_2)$ allows for determining the dynamically enforced condition of homokinetism. After the trigonometric considerations we state that the condition is satisfied for the following dependence:

$$\alpha = \frac{\delta}{2} \tag{21}$$

The equations (12) and (21) are analogical. Therefore the interpretation of the obtained result for the sufficient condition is the same as for the necessary condition.

5. The kinematic values characterizing the intermediate system motion of the Birfield–Rzeppa joint

The cage along with the balls is the intermediate element of the Birfield–Rzeppa joint. The system is modeled in the form of a clamping ring P and the rings (e.g. p. A). Point A determines the position of the ring, thus it is linked to one of the balls. We assume the point does not relocate towards the cage while transferring the motion from drive shaft (1) onto the driven shaft (2).

The position function

The position function $f(\phi_1)$ of the system consisting of the drive shaft (1) and the clamping ring P is determined by the dependence of the drive shaft rotation angle ϕ_1 on the clamping ring rotation angle $P\phi_3$:

$$\phi_3 \rightleftarrows f(\phi_1) \tag{22}$$

The position of point A is determined by the vector $\vec{r}_3$. The vector is defined explicitly by the dependencies (7) and (8). If the conditions (12) and (21) are fulfilled and the position of the vector $\vec{r}_3$ will be dependent solely on the rotation angle of the clamping ring $P\phi_3$, we will receive the following dependencies in the coordinate system $0x_1y_1z_1$:

$$\vec{r}_3\left(r_{3x_1}, r_{3y_1}, r_{3z_1}\right) \tag{23}$$

$$r_{3x_1} = r_3\, sin\,\phi_3\; r_{3y_1} = -r_3 \sin\frac{\delta}{2}\cos\varphi_3\; r_{3z_1} = r_3\, cos\frac{\delta}{2} cos\,\phi_3$$

https://doi.org/10.14669/AM/177006

Taking into consideration dependencies (8) and (23) and the dot product determined by the equation (24):

$$\vec{r}_1 \bullet \vec{r}_3 = 0 \tag{24}$$

We receive an analytical equation of geometrical constraints imposed on the motion of the driver shaft and the camping ring P along with the rings:

$$tg\phi_3 = cos\frac{\delta}{2} tg\phi_1 \tag{25}$$

Hence:

$$\phi_3 = arctg\left(cos\frac{\delta}{2} tg\phi_1\right) = f(\phi_1) \tag{26}$$

The equation (26) is the positon function of the system consisting of a driver shaft (1) and the camping ring P along with the rings.

Transmission function

Having the equations (22) and (26) it is possible to determine the transmission function $f'(\phi_1)$ of the system composed of the driver shaft (1) and the clamping ring P along with the rings:

$$\dot{\phi}_3 \rightleftarrows f'(\phi_1)\dot{\phi}_1 \tag{27}$$

Thus:

$$\dot{\phi}_3 \rightleftarrows \frac{cos\frac{\delta}{2}}{1-sin^2\frac{\delta}{2}sin^2\phi_1}\dot{\phi}_1 \tag{28}$$

where:
$\dot{\phi}_1$ – angular velocity of the drive shaft rotation (1)
$\dot{\phi}_3$ – angular velocity of the clamping ring P rotation with rings

Hence:

$$f'(\phi_1) \rightleftarrows \frac{cos\frac{\delta}{2}}{1-sin^2\frac{\delta}{2}sin^2\phi_1} \tag{29}$$

The equation (29) is the function of transmission of the system consisting of a drive shaft (1) and the clamping ring P along with the rings.

https://doi.org/10.14669/AM/177006

The second function of position

Having the equation (27) and (28) it is possible to determine the second function of position $f''(\phi_1)$ of the system consisting of a drive shaft (1) and the clamping ring P along with the rings:

$$\ddot{\phi}_3 \rightleftarrows f''(\phi_1)\dot{\phi}_1^2 + f'(\phi_1)\ddot{\phi}_1 \tag{30}$$

If we assume that the drive shaft rotates with uniform motion then:

$$\dot{\phi}_1 = const \Rightarrow \ddot{\phi}_1 = 0 \tag{31}$$

And the equation (30) takes the form of:

$$\ddot{\phi}_3 \rightleftarrows f''(\phi_1)\dot{\phi}_1^2 \tag{32}$$

Thus:

$$\ddot{\phi}_3 \rightleftarrows \frac{cos\frac{\delta}{2}sin^2\frac{\delta}{2}sin\,2\phi_1}{\left(1-sin^2\frac{\delta}{2}sin^2\,\phi_1\right)^2}\dot{\phi}_1^2 \tag{33}$$

where:

$\ddot{\phi}_1$ – angular acceleration of the drive shaft (1)

$\ddot{\phi}_3$ – angular acceleration of the clamping ring P and the rings

$$f''(\phi_1) \rightleftarrows \frac{cos\frac{\delta}{2}sin^2\frac{\delta}{2}sin\,2\phi_1}{\left(1-sin^2\frac{\delta}{2}sin^2\,\phi_1\right)^2} \tag{34}$$

The equation (34) is the second position function of the system consisting of a drive shaft (1) and the clamping ring P along with the rings.

Motion trajectory of point A

The position of point A is determined by vector $\vec{r}_3$. The vector is identified explicitly by dependencies (7) and (8). If the conditions (12) and (21) are fulfilled and the vector $\vec{r}_3$ position is dependent solely on the rotation angle of the drive shaft (1) ϕ_1, then we obtain the following dependencies in the coordinate system $0x_1y_1z_1$:

$$\vec{r}_3\left(r_{3x_1}, r_{3y_1}, r_{3z_1}\right) \tag{35}$$

$$r_{3x_1} = r_3\frac{cos\frac{\delta}{2}sin\,\phi_1}{\sqrt{1-sin^2\frac{\delta}{2}sin^2\,\phi_1}} \quad r_{3y_1} = -r_3\frac{\sin\frac{\delta}{2}\cos\varphi_1}{\sqrt{1-\sin^2\frac{\delta}{2}\sin^2\varphi_1}} \quad r_{3z_1} = r_3\frac{cos\frac{\delta}{2}cos\,\phi_1}{\sqrt{1-sin^2\frac{\delta}{2}sin^2\,\phi_1}}$$

https://doi.org/10.14669/AM/177006

where:

$$\phi_1 = \dot{\phi}_1 t + \phi_{10}$$

The dependencies (35) are finite motion equations of point A. It is the parametric form of equations determining the motion trajectory of the point A.

Linear velocity of point A

Taking into consideration the dependencies (35) and (36)

$$\vec{V}_A = \frac{d\vec{r}_3}{dt} \tag{36}$$

We receive the vector coordinates of the linear velocity of point A in the coordinate system $0x_1y_1z_1$:

$$\vec{V}_A\left(V_{Ax_1}, V_{Ay_1}, V_{Az_1}\right) \tag{37}$$

$$V_{Ax_1} = \frac{\dot{\phi}_1 r_3 \cos\frac{\delta}{2}\cos\phi_1}{\left(1-\sin^2\frac{\delta}{2}\sin^2\phi_1\right)^{\frac{3}{2}}} V_{Ay_1} = \frac{\dot{\varphi}_1\, r_3 \sin\dfrac{\delta}{2}\cos^2\dfrac{\delta}{2}\sin\varphi_1}{\left(1-\sin^2\dfrac{\delta}{2}\sin^2\varphi_1\right)^{\frac{3}{2}}} V_{Az_1} = \frac{\dot{\phi}_1 r_3 \cos^3\frac{\delta}{2}\sin\phi_1}{\left(1-\sin^2\frac{\delta}{2}\sin^2\phi_1\right)^{\frac{3}{2}}}$$

Tangential acceleration of point A

Taking into consideration the dependence (33) and examining the components of vector $\vec{\dot{\phi}}_3$, (35) and (38)

$$a_{A\tau} = \vec{\dot{\phi}}_3 \times \vec{r}_3 \tag{38}$$

We obtain acceleration vector coordinates of the tangential point A in the coordinate system $0x_1\,y_1\,z_1$:

$$\vec{a}_{A\tau}\left(a_{A\tau x_1}, a_{A\tau y_1}, a_{A\tau z_1}\right) \tag{39}$$

$$a_{A\tau x_1} = \frac{\ddot{\phi}_3 r_3 \cos\phi_1}{\sqrt{1-\sin^2\frac{\delta}{2}\sin^2\phi_1}} a_{A\,y_1} = \frac{\ddot{\varphi}_3 r_3\ \cos\dfrac{\delta}{2}\sin\dfrac{\delta}{2}\sin\varphi_1}{\sqrt{1-\sin^2\dfrac{\delta}{2}\sin^2\varphi_1}} a_{A\tau z_1} = \frac{-\ddot{\phi}_3 r_3 \cos^2\frac{\delta}{2}\sin\phi_1}{\sqrt{1-\sin^2\frac{\delta}{2}\sin^2\phi_1}}$$

Normal acceleration of point A

Taking into consideration the dependence (28) and examining the components of the vector $\vec{\dot{\phi}}_3$, (37) and (40)

$$a_{An} = \vec{\dot{\phi}}_3 \times \vec{V}_A \tag{40}$$

https://doi.org/10.14669/AM/177006

We obtain the coordinates of the normal acceleration vector of point A in the coordinate system $0x_1y_1z_1$:

$$\vec{a}_{A\tau}\left(a_{Anx_1}, a_{Any_1}, a_{Anz_1}\right) \tag{41}$$

$$a_{Anx_1} = \frac{-\dot{\phi}_3^2 r_3 \cos\frac{\delta}{2}\sin\phi_1}{\sqrt{1-\sin^2\frac{\delta}{2}\sin^2\phi_1}} \quad a_{Any_1} = \frac{\dot{\varphi}_3^2 r_3 \sin\frac{\delta}{2}\cos\varphi_1}{\sqrt{1-\sin^2\frac{\delta}{2}\sin^2\varphi_1}} \quad a_{Anz_1} = \frac{-\dot{\phi}_3^2 r_3 \cos\frac{\delta}{2}\cos\phi_1}{\sqrt{1-\sin^2\frac{\delta}{2}\sin^2\phi_1}}$$

6. Numerical simulation

The exemplary results of numerical simulations determining the variability course of the transmission function $f'(\phi_1)$ and the second position function $f''(\phi_1)$ characterizing the intermediate element motion of the homokinetic Birfield-Rzeppa joint will be presented.

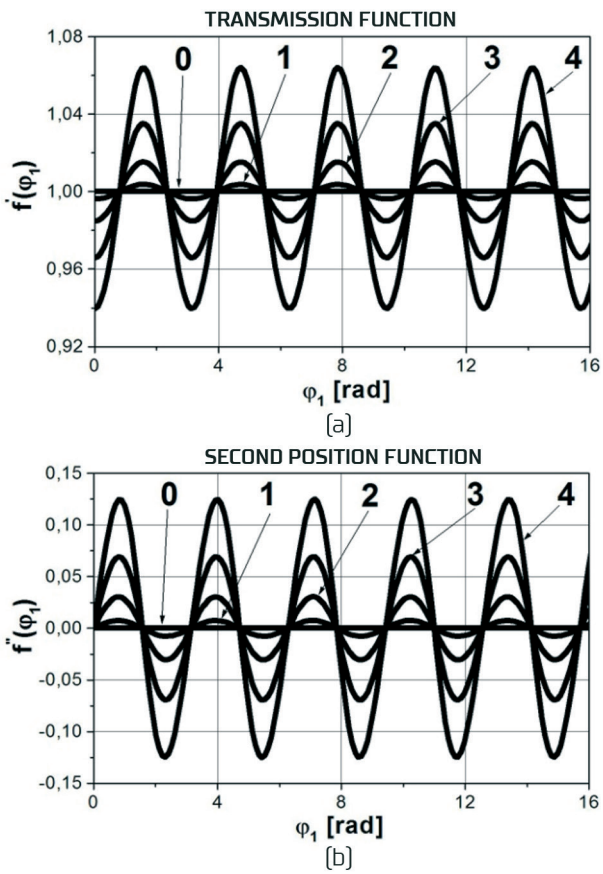

Fig. 3. (a) Variability course of the transmission function $f'(\phi_1)$; (b) variability course of the second position function $f''(\phi_1)$

https://doi.org/10.14669/AM/177006

Designation in Figure 3:

$$0\text{-}\delta = 0, \quad 1\text{-}\delta = 10, \quad 2\text{-}\delta = 20, \quad 3\text{-}\delta = 30, \quad 4\text{-}\delta = 40, \quad \delta \rightarrow [deg]$$

7. Conclusions

The Birfield–Rzeppa joint is homokinetic if the conditions (12) and (21) are fulfilled. The equations (12) and (21) are analogical. Therefore the interpretation of the obtained result for the sufficient condition is the same as for the necessary condition. It means that the intermediate element in the form of a cage along with the balls should rotate in the constant velocity plane. The uniform rotary motion of the drive shaft (1) leads to the excitation of vibrations of the intermediate element. The kinematic vibrations are forced by the geometric constraints imposed on the mechanism (25). Having the variability course of the transmission function $f'(\phi_1)$ (29) and the second position function $f''(\phi_1)$ (34) (e.g. Figure 3) one can determine the kinematic values characterizing the motion of the cage and balls, e.g. (28), (33), (37), (39) and (41). The fluctuation of values in time is characteristic of these values courses. As the angle of refraction of the shaft axes increases, the level of these fluctuations increases significantly. If the gear ratio function and the second clutch position function introduce fluctuations in the values of the angular velocity and angular acceleration of the basket and the balls, vibrations are generated in the joint.

The change of the articulated joint structure is justified and therefore the intermediate element vibrations cannot be eliminated. Thus the examination should be focused on the control of the generated vibrations [2, 3, 8]. One of the logical structural solutions is the introduction of an element reducing the disturbance of the driven shaft as in Figure 4. The article does not present an analysis aimed at reducing vibrations. Only the need for its use in the case of serious disorders has been demonstrated. Presenting the application of a system that can control the resulting vibrations requires additional analysis. Such considerations are so extensive that they require the editing of an independent article.

https://doi.org/10.14669/AM/177006

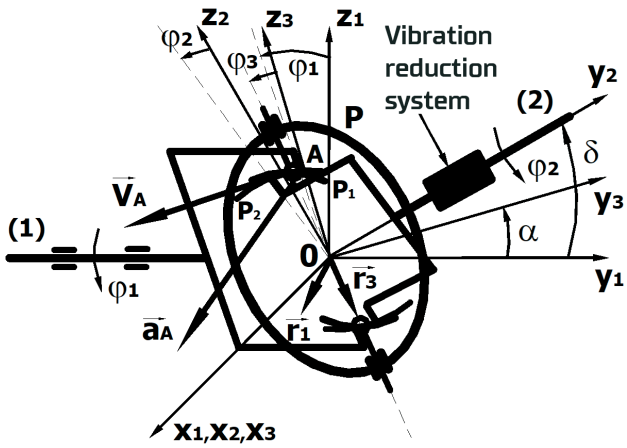

Fig. 4. Vibration reduction system – Birfield–Rzeppa joint model

8. References

[1] Cirelli M., Giannini O., Cera M., De Simoni F., Valentini P.P., Pennestrì E.: The mechanical efficiency of the Rzeppa transmission joint. Mechanism and Machine Theory. 2021, 164, 104418, DOI: 10.1016/j.mechmachtheory.2021.104418.

[2] Crocker M.J.: Handbook of Noise and Vibration Control. John Wiley & Sons. Canada, 2007.

[3] De Silva C.W.: Vibration Fundamentals and Practice. Taylor & Francis Group. Boca Raton, London, New York, 2007.

[4] Gabryelewicz M.: Podwozia i nadwozia pojazdów samochodowych. WKiŁ. Warszawa, 2011.

[5] Feng H., Yin Z., Shangguan W–B., Li X., Luo Y.: Analysis and optimization for contact forces and transmission efficiency of an automotive ball joint. Proceedings of the Institution of Mechanical Engineers, Part D: Journal of Automobile Engineering. 2020, 234(14), 3207–3223, DOI: 10.1177/0954407020952583.

[6] Hildebrandt W., Horst J., Rickell R.A.: New constant velocity fixed joints for front-wheel drivecars. ATZ Worldw. 2006, 108(2–4), DOI: 10.1007/BF03224822.

[7] Hildebrandt W., Schmahl C., Reith D. Gleichlaufgelenke für den modernen Triebstrang: Ein Technologieüberblick unter besonderer Berücksichtigung ihres Einflusses auf den Fahrzeug-Energieverbrauch. Mintzlaff, Strohe (Hg.): Triebstränge in Fahrzeugen: Pkw, Motorräder, Nutzfahrzeuge und mobile Arbeitsmaschinen. Haus der Technik Fachbuch, Bd. 2016, 140, 124–137, expert Verlag.

[8] Inman D.J.: Vibration with Control. John Wiley & Sons. The Atrium, Southern Gate, Chichester, West Sussex PO19 8SQ, England 2006.

[9] Kimata K., Nagatani H., Imoto M., Kohara T.: Numerical Analyses and Experiments on the Characteristics of Ball-Type Constant-Velocity Joints. JSME International Journal Series C Mechanical Systems, Machine Elements and Manufacturing. 2004, 47(2), 746–754, DOI: 10.1299/jsmec.47.746.

[10] Pennestrì E., Rossi V., Salvini P., Valentini P.P., Pulvirenti F.: Review and kinematics of Rzeppa-type homokinetic joints with straight crossed tracks. Mechanism and Machine Theory. 2015, 90, 142–161, DOI: 10.1016/j.mechmachtheory.2015.03.009.

[11] Pennestrì E., Valentini P.P.: Kinematic design and multi-body analysis of Rzeppa pilot-lever joint. Proceedings of the Institution of Mechanical Engineers, Part K: Journal of Multi-body Dynamics. 2008, 222(2), 135–142, DOI: 10.1243/14644193JMBD131.

[12] Shi S., Chu H., Qiu X., Zhou Y.: Novel double-deck Rzeppa constant velocity joint with large operating angle: Mechanism configuration and kinematic characteristics analysis. Proceedings of the Institution of Mechanical Engineers, Part C: Journal of Mechanical Engineering Science. 2023, 105407, DOI: 10.1177/09544062231166799.

[13] Simpson M., Dolatabadi N., Rahmani R., Morris N., Jones D., Craig Ch.: Multibody Dynamics of Cross Groove Constant Velocity Ball Joints for High Performance Racing Applications. Mechanism and Machine Theory. 2023, 188, DOI: 10.1016/j.mechmachtheory.2023.105407.

[14] The materials made available by the Löbro company, Gleichlauf-Festgelenke und Verschiebegelenke. München, 2008.

[15] The materials made available by the Löbro company, Gleichlauf Gelenkwellen in Antrieben des Maschinenbaus. München 2008

[16] Wang G., Qi Z., Zhang Z.: Kinematic Analysis and Simulation of the Steel Balls for Rzeppa Constant Velocity Joint. Chinese Journal of Mechanical Engineering. 2012, 48(3), 147–153, DOI: 10.3901/JME.2012.03.147.

[17] Watanabe K., Matsuura T.: Kinematic Analyses of Rzeppa Constant Velocity Joint by Means of Bilaterally Symmetrical Circular-Arc-Bar Joint. The Proceedings of the Machine Design and Tribology Division meeting in JSME. 2006, 6, DOI: 10.1299/jsmemdt.2006.6.131.

[18] Valentini P.P.: Effects of the dimensional and geometrical tolerances on the kinematic and dynamic performances of the Rzeppa ball joint. Proceedings of the Institution of Mechanical Engineers, Part D: Journal of Automobile Engineering. 2014, 228(1), 37–49, DOI: 10.1177/0954407013505745.